Scale invariants in the preparation of reverse high internal phase ratio emulsions

Anna May-Masnou*, Montserrat Porras, Alicia Maestro, Carme González, José María Gutiérrez

Departament d'Enginyeria Química, Facultat de Química, Universitat de Barcelona

Martí i Franquès, 1-11, 08028, Barcelona, Catalunya, Spain.

*anna.may@ub.edu, Tel : +34 9340 39789, Fax: +34 9340 21291

Abstract

Reverse high internal phase ratio emulsions (HIPRE) are prepared with the system water/Span80/dodecane to identify the influence of the process variables on droplet size and polydispersity, and to study the influence of the process scale-up. After discussing the most common scale invariants used in emulsification processes, we prepare emulsions at two different scales following a complete factorial experimental design. Using the empirical models obtained with the statistical analysis of the results, we determine the scale invariants for the system. Results from a previous study indicated that the scale invariant for the preparation of HIPRE could be the stirring rate. However, the results obtained in this work show that the scale invariant, based on droplet size, could change depending on the conditions of emulsification. Only when the stirring rate is high enough (> 1500 rpm), or when the surfactant-to-oil ratio is high and the total addition time low, the scale invariant is indeed the stirring rate. The elevated shear stress inside the mixer when the stirring rate is high is responsible of the small droplet size obtained on both scales. However, for other values of the process variables, the scale-invariant can be expressed as $N \cdot D^{\alpha}$, where $0 < \alpha < 0.5$, and depends on other two factors: the addition flow rate of dispersed phase or addition time, and the surfactant-to-

Published in: Chemical Engineering Science, Volume 101, 20 September 2013, Pages 721–730

oil ratio. We propose a methodology to determine these scale invariants and to calculate the threshold values of surfactant-to-oil ratio and addition flow rate from which the stirring rate is the scale invariant (when $\alpha \to 0$).

Keywords: Scale-up, Reverse high internal phase ratio emulsion, Scale invariant, Droplet size, Stirring rate.

1. Introduction

Scale-up from experimental laboratory equipment to industrial plant size is one of the crucial issues in the field of industrial process design. The processes working with low-viscosity Newtonian fluids are, usually, directly scalable. However, the scaling-up of processes involving high-viscosity non-Newtonian fluids is far more complicated, since fluid properties, like viscosity, and flow conditions can vary drastically during the process (Wilkens et al., 2003). This is the case of emulsion manufacturing. Moreover, the final quality and properties of an emulsion are very dependent on the process variables, so a little change in the stirring rate, in the way of adding the components or in the vessel size can result in changes in the product quality, apart from a raw material, time and economical loss. The scale-up analysis of these processes and the study of the effect of process variables on the emulsion quality are necessary in order to predict what will happen at industrial scale and to optimize the process, saving money and time in unproductive tests. However, not many studies are available (Baby et al., 2008; Capdevila et al., 2010; Galindo-Rodríguez et al., 2005; Mitri et al., 2012; Solè et al., 2010), most of them concerning nano-emulsions (Galindo-Rodríguez et al., 2005; Mitri et al., 2012; Solè et al., 2010). Highly-concentrated emulsions have some special features that make the study of their scaling-up different from nano-emulsions and crucial if their production wants to be implemented at industrial scale. Due to the extremely high volume fraction of the dispersed phase (> 0.74), it is important to favor droplet breakup and, at the same time, to avoid droplet coalescence, in order to obtain a minimum polydispersity and maximum emulsion stability, with the smallest droplet size as possible. The amount of surfactant plays an important role on the stabilization of the

Published in: Chemical Engineering Science, Volume 101, 20 September 2013, Pages 721–730

58 emulsion, although its preparation method is also determining. One of the main keys of
59 this study is to study the scale-up of highly-concentrated emulsion formation and to
60 determine which are the variables that have to be kept constant at both scales in order to
61 obtain emulsions with the same properties i.e., determine the scale invariants.
62
63 **1.1 Scale invariants**
64 To perform a successful scale-up, there are many empirical scale-up criteria or simple
65 *rules of thumb* based on the experience, which involve the formulation of mathematic
66 correlations using experimental data. These, along with similarities and dimensional
67 analysis, constitute the scale-up model of the process, which requires enough data
68 available to validate it. Since emulsion formation can be assimilated to an isotherm
69 mixture of two fluids (Capdevila et al., 2010; Okufi et al., 1990; Podgórska and
70 Baldyga, 2001; Wilkens et al., 2005), the scale-up criteria for mixing and agitation are
71 discussed here, including the dimensionless numbers – despite their rarely successful
72 scale-up (Zlokarnik, 1998).
73
74 For stirred vessels, the impeller Reynolds number ($\mathrm{Re}_i = \rho \cdot N \cdot D^2 / \mu$) determines if the
75 flow is laminar ($\mathrm{Re_i} < 10$), turbulent ($\mathrm{Re_i} > 10000$) or transitional. $\mathrm{Re_i}$ is obtained when
76 applying dimensional analysis to the scale-up of mixing vessels (Bird et al., 1964), so it
77 seems an appropriate criterion, as it includes the most representative variables that
78 affect the final product, like the stirring rate (N), the impeller diameter (D), the fluid
79 density (ρ) and fluid viscosity (μ). However, it does not give information of the degree
80 of mixing or of the intensity of turbulence. To maintain the $\mathrm{Re_i}$ constant at both scales,
81 the stirring rate at the large-scale (N_2) needs to be equal to the stirring rate at small-scale

multiplied by the square of the inverse geometric ratio of impeller diameters: $N_2 = N_1 \cdot (D_1/D_2)^2$, considering that the same model material is used in both scales (implying constant density and viscosity). This, along with geometric similarity, implies that the stirring rate at the large scale should be one fourth of the stirring rate at small scale, which is usually not enough if a turbulent flow wants to be achieved at industrial scale to ensure an efficient mixing. In order to keep Re_i constant, it is suggested to use a less viscous model fluid at small scale (Bird et al., 1964), and then avoid working at high rotational speeds. The same solution is proposed by Bakker and coworkers (Bakker and Gates, 1995) in order to maintain the same flow pattern in both scales for viscous liquid mixing applications. However, in spite of the efforts made to keep Re_i constant, it is not always the best scale-up criterion. A study (Johnson, 1967) found that this criterion did not result in equal mixing time at both scales in the mixing of viscous liquids using a turbine impeller; and others (Taylor et al., 2005) states that, in general, the Reynolds number in itself is never a proper scale-up criterion, and that it invariably increases with scale-up; Gutiérrez et al. (Gutiérrez et al., 2008) considered that keeping Re_i constant in the scale-up of nano-emulsions would imply too high stirring rates at small scale to reach the Re_i used in practical industrial applications, so they used the tip speed velocity $(v = \pi \cdot N \cdot D)$ as scale-up invariant, together with the total addition time. In their study, when the Reynolds number was constant, there was no correspondence between scales in the final product, as it was suggested that mixing was not achieved due to a high turbulence or strong eddies. Due to the extreme viscosity of the system in the intermediate stages, where a liquid crystal phase was formed, viscous forces were more important than inertial forces; the fluid was moved along with the stirrer and it dragged the rest of the fluid with it. The stirrer geometry and the inhomogenities of the

system helped the mixing. Baldyga et al. (Baldyga et al., 2001), also affirmed that scaling-up at constant tip speed in the formation of nano-emulsions resulted in identical droplet size for the large droplets at both scales, although depending on the duration of agitation, bigger droplets could be obtained in the larger scale tanks. So, apart from the tip speed, the addition time should also be considered.

In fact, equal tip speed or velocity in both scales should assure that all the parts of the fluid should be moving equally at both scales and with no stagnant areas. According to Wilkens et al. (Wilkens et al., 2003), this is a common criterion associated to industrial stirrers and phenomena sensitive to shear stress, like in emulsions, where it is interesting to control droplet size. Moreover, this criterion is recommended when a response variable of an emulsion (for example droplet size or some rheological parameter) is clearly correlated with tip speed. Equal tip speed implies that the large-scale stirring rate is equal to the small-scale stirring rate multiplied by the inverse geometric ratio of the impeller diameters: $N_2 = N_1 \cdot (D_1/D_2)$, so if the diameter is doubled, the stirring rate should be reduced by a factor of two. When scaling-up with this criterion, the Reynolds number is increased, while power/volume (P/V) is decreased and torque/volume (T/V) remains constant with increasing scale. Okufi et al. (Okufi et al., 1990) studied the scale-up of liquid-liquid dispersions in three different vessels with geometric similarity, varying tip speed and volume fraction of dispersed phase. At a constant tip speed between scales, they found no variation in the response variables, so they affirm that this criterion is valid for scaling-up systems like the one they studied. The response variable chosen was the surface area of dispersion (a_v), which is defined as the interfacial area of dispersed phase (a_d) per unit volume of the whole dispersion

($V_t = V_d/\phi$, where ϕ is the dispersed phase volume fraction and V_d the volume it occupies). Taking $a_d = n \cdot \pi \cdot d_{32}^2$ and $V_d = n \cdot \pi \cdot d_{32}^3/6$ (n is the number of droplets, d_{32} the Sauter mean diameter): $a_v = a_d/V_t = 6 \cdot \phi/d_{32}$, so a_v can be calculated knowing d_{32} and ϕ. Johnson et al. (Johnson, 1967) studied three different stirrers to mix viscous fluids with a turbine, and found that constant tip speed was the best scale invariant for miscible liquids and small changes in scale. The torque per unit volume is an important mixing characteristic that also represents mixing intensity in terms of fluid velocities (Dickey, 2005), since it is similar to momentum transfer, which is related to the motion created by the impeller. Torque (T) is defined as the ratio between power and rotational speed ($T=P/N$). In turbulent conditions and geometric similarity, this criterion results in the same expression as equal tip speed. In this case, the torsion capacity of the stirrer is related directly with its size (Wilkens et al., 2003).

The Froude number for a stirred tank ($Fr = N^2 \cdot D/g$) is also a dimensionless parameter obtained when doing dimensional analysis in mixing applications (Bird et al., 1964). If the Froude number is constant at both scales, the rotational speed at the large-scale is equal to the rotational speed at small-scale multiplied by the square of the inverse geometric ratio of impeller diameters: $N_2 = N_1 \cdot (D_1/D_2)^{1/2}$, so if the diameter in the large scale is two times the diameter of the small scale, then the stirring rate will be 0.7 times the small scale stirring rate. Performing dimensional analysis to the scale-up of stirred tanks, it appears that the Reynolds number and the Froude number have to be constant at both scales if dynamic similarity is required. However, it is physically impossible to maintain $N \cdot D^2$ (Re) and $N^2 \cdot D$ (Fr) constant at the same time with the same

153 model material, although some authors (Bakker and Gates, 1995) affirm that when
154 studying vortex formation, this should be so, by using different viscosity fluids at both
155 scales, as Fr takes into account the gravitational forces of the fluid, and is important
156 when vortex are formed in the emulsion. In the case of high-viscosity fluids, like
157 HIPRE, the inherent high viscosity prevents the formation of vortex, and the
158 significance of this number almost disappears (Capdevila et al., 2010). Moreover, the
159 use of this criterion leads to overdimensioned systems and, as a consequence, it is not an
160 economical criterion (Wilkens et al., 2003).
161
162 The power number, also known as Newton number, a dimensionless parameter
163 expressed as $N_p = P/\rho \cdot N^3 \cdot D^5$, where P is the power, represents the ratio of pressure to
164 inertia forces and is also widely used in mixing applications (Angst and Kraume, 2006;
165 Briceño et al., 2001; Houcine et al., 2000; Landin et al., 1996; Podgórska and Baldyga,
166 2001; Rewatkar and Joshi, 1991). This number depends essentially on the impeller
167 geometry, so for geometric similarity between the two scales, the power number will be
168 the same at both scales in turbulent conditions (large Re). To maintain the power
169 number constant, the large scale stirring rate needs to be 0.315 times the small-scale
170 stirring rate if the diameter is increased by a factor of two. Then, the power
171 requirements in both systems will also change proportionally to these variables.
172
173 The energy intensity, expressed as power per unit volume (*P/V*), is the most used scale-
174 up criterion, as it is easy to understand in mixing applications and the most practical.
175 Moreover, it correlates well with mass transfer characteristics (Wilkens et al., 2003).
176 This criterion represents dynamic similarity under negligible viscous forces, i.e., in

177 turbulent regime (Re >10000), and when gravitational forces have no effect. It is usually
178 used in dispersions (Okufi et al., 1990). The criterion of *P/V* is equal to maintaining
179 $N^3 \cdot D^2 = cnt$, which means that the large-scale stirring rate is equal to the small-scale
180 stirring rate multiplied by the inverse geometric ratio of the impeller diameters at the 2/3
181 power: $N_2 = N_1 \cdot (D_1/D_2)^{2/3}$. However, this is only valid in turbulent flow, when N_p
182 remains constant. Although some authors (Zlokarnik, 1998) affirm that this criterion is
183 adequate for gas/liquid systems and liquid/liquid dispersions when the power is equally
184 distributed in all the tank volume, there are many authors (Johnson, 1967; Okufi et al.,
185 1990) that support that this criterion results in an overdimension of the equipment in
186 industrial scale. Bourne et al. (Bourne and Yu, 1994) applied the *P/V* criterion for
187 reactions in stirred tanks and found that, in general, this was not a good matching
188 because of the variations of the trajectory of the reaction zone during scale-up, and
189 found no simple scale-up criterion for micromixing in stirred tank reactors. In the case
190 of emulsion formation with the continuous addition method, the parameter *P/V* is
191 difficult to control, as the batch volume increases with time, and also the power input,
192 due to the change in viscosity of the emulsion.
193
194 The stirring rate (*N*), also referred as rotational velocity or impeller speed is proposed to
195 be the scale-up criterion for highly-concentrated emulsions in our previous study
196 (Capdevila et al., 2010). The emulsions were prepared at two different scales with
197 geometric similarity. Considering that the viscosity of the system was high, the scale-up
198 was first performed maintaining the tip speed constant instead of the Reynolds number,
199 based on the results from Solè et al. (Solè et al., 2010). However, in contrast to the study
200 with nano-emulsions, the highly-concentrated emulsion droplets formed in the large

tank were bigger than the ones formed in the small-scale vessel, so in this case, the tip speed did not constitute a convenient scale-up invariant; neither would Reynolds number, as it would imply even a smaller mixing rate at the big scale. This was supported by the fact that, by keeping the tip speed constant, the stirring rate was lower at the higher scale involving an increase in droplet size. However, a correspondence appeared between the two scales in the points in which the stirring rate was the same. Since in the emulsification process to form highly-concentrated emulsions, a critical aspect is the creation of interfacial area (droplet breakup to form smaller droplets) rather than the degree of mixing, the stirring rate, directly related to the shear stress, τ, is important. The shear stress τ is responsible to deform and breakup the droplets and is related to the shear rate $\left(\tau = \eta_{av} \cdot \dot{\gamma}\right)$ by the average viscosity of the emulsion. This shear rate is related by many authors (Alvarez, 2006; Alvarez et al., 2010; Anne-Archard et al., 2006; Bakker and Gates, 1995; Thakur et al., 2004) with the stirring rate using the Metzner-Otto equation (Metzner and Otto, 1957), ($\dot{\gamma} = K \cdot N$), as it is a velocity gradient along the radius of the impeller, where the proportionality constant (K) depends on the type of the impeller and on the geometry of the system used. For this reason, the stirring rate, which depends on the shear rate, could seem to determine the droplet size. However, no further experiments were performed to confirm what was suggested in this previous study (Capdevila et al., 2010).

The stirring rate was found to be a proper scale-up invariant in other studies, for example for stirred tank reactors where fast reactions take place, although not supported by all authors (Taylor et al., 2005). This criterion is also supported by Galindo-Rodríguez et al. (Galindo-Rodríguez et al., 2005), for the scaling-up of nano-emulsions.

225 Moreover, it was pointed out that apart from *N* and the geometric similarity, the
226 dynamic similarity had to be taken into account when scaling-up and this was achieved
227 by maintaining constant the specific power input of the stirrer (*P/V*). However, the
228 droplet size in the pilot-scale was always smaller than in the lab-scale, for a same value
229 of *N*. The same conclusion, in the micrometric range was obtained by Baldyga et al.
230 (Baldyga et al., 2001): they saw a slow drift towards smaller drops when agitation was
231 maintained, as well as smaller drops and faster breakup when scaling-up at constant
232 power per unit volume (*P/V*). According to these statements, neither *N* nor *P/V*, were
233 adequate scale-up invariants, because the same emulsion drop sizes were not obtained
234 when maintaining them constant.
235
236 **1.2 The power law relationship**
237 Most of the criteria exposed in the previous section can be summarized with an
238 expression in which the stirring rate in the higher scale is given by the one at the
239 smaller scale multiplied by the ratio between the two impeller diameters elevated at an
240 exponent $\left(N_2 = N_1 \cdot (D_1/D_2)^{\alpha}\right)$. This concept is similar to the scale-up approach
241 considered by Gorsky (Gorsky, 2006), based on geometric similarities and using a
242 power law relationship: $X_2 = X_1 (1/R)^{\alpha}$. In this equation, X_2 is an unknown variable in
243 the large scale calculated from X_1, R is the geometric scaling factor, which is a
244 geometric relation between scales (for example D_2/D_1), α is the power law exponent,
245 determined empirically or theoretically, and the indices *1* and *2* indicate the small (or
246 lab) scale and the large (or industrial) scale, respectively. The power law exponent has
247 a physical meaning, as described in Table 1 (adapted from Levin (Levin, 2006)), which
248 summarizes what has been discussed here. In the first column, the common scale

invariants used in typical stirred tank reactors mixing operations are shown. The second column indicates which is the relation that has to be kept constant at all scales, in terms of N and D, and the equation in the third column corresponds to the stirring rate in the bigger scale (N_2), given the stirring rate in the smaller scale (N_1) and both impeller diameters (D_1 and D_2). It can be observed that P/V is shown to be equivalent to the power law scale-up approach with a power law exponent equal to $\alpha = 2/3$, as the power requirement is proportional to $N^3 \cdot D^5$, and the tank volume, due to geometric similarity, is a fixed multiple of impeller diameter, D^3. Moreover, as the amount of power per unit volume is directly related to the liquid turbulence on the interface, the mass transfer rates will also be dependent on this parameter. The Froude number is related to vortex formation, which is, at the same time, related to the liquid surface motion, as can be observed in the table when $\alpha = 1/2$. When the scale invariant is N, the power law exponent is 0, whereas if the scale invariant is the tip speed, the exponent is equal to 1.

Table 1. Scale-up invariants and physical meaning of the power law exponent. Notation: *N*, stirring rate; *D*, impeller diameter; *t*, mixing time; *1* and *2* for the small and large scale. Adapted from (Levin, 2006).

Constant parameter	Constant relation	N_2	Power law exponent	Physical meaning
Re	$N \cdot D^2$	$N_1 \cdot (D_1/D_2)^2$	*2*	Equal fluid flow regime
We	$N^2 \cdot D^3$	$N_1 \cdot (D_1/D_2)^{3/2}$	*3/2*	Equal stress to form same size droplets
T/V	$N^2 \cdot D^2$	$N_1 \cdot (D_1/D_2)$	*1*	Equal liquid motion (fluid velocity) or tip speed velocity ($v=N \cdot D$) or torque per unit volume (*T/V*)
v	$N \cdot D$	$N_1 \cdot (D_1/D_2)$	*1*	
P/V	$N^3 \cdot D^2$	$N_1 \cdot (D_1/D_2)^{2/3}$	*2/3*	Equal mass transfer rates or equal power per unit volume (*P/V*)
Fr	$N^2 \cdot D$	$N_1 \cdot (D_1/D_2)^{1/2}$	*1/2*	Equal surface motion
N	*N*	$N_1 \cdot (D_1/D_2)^0$	*0*	Equal shear rate

Once having discussed the scale invariants used in mixing applications and emulsion preparation, the goal of this study is to confirm or to disprove that the stirring rate is the scale invariant for the scale-up and preparation of reverse highly-concentrated emulsions using water/Span 80/dodecane and, in the case it is not, identify the threshold values of the process variables from which it is valid. At the same time, identify those factors that have a major influence on the emulsion properties and propose a general scale-up methodology for the preparation of this type of emulsions.

2. Experimental section

2.1 Materials

Reverse highly-concentrated emulsions consisted in a continuous phase of dodecane (99.5 %) and Span80® (HLB = 4.3), both from Sigma Aldrich and used as received, at different surfactant-to-oil ratios (*S/O)*. Milli-Q water was used as dispersed phase with a constant volume fraction of 0.90.

2.2 Determination of the phase diagrams

To determine the phase diagram of the system water/Span80/dodecane, the required amounts of each product were weighed in clean and dry glass tubes. The tubes were sealed and the mixture was homogenized using a Vortex stirrer and left in a water-bath at 25 ºC until equilibration was reached. The determination of the phases was performed by visual observation under polarized optical microscopy (POM) and by analyzing the turbidity, texture and viscosity of the samples.

Published in: Chemical Engineering Science, Volume 101, 20 September 2013, Pages 721–730

2.3 Preparation of the emulsions and determination of energy consumption

Emulsions were prepared in jacketed stirred-tank reactors following a 2-step batch process. The system (Figure 1) consists of a glass jacketed vessel and a three-level P-4 pitched blade impeller, to cover all the vessel height and provide a good emulsification. A peristaltic pump (ISMATEC MCP) provided a constant addition flow rate of dispersed phase. A thermostatic bath (HAAKE F6-C25) is used to maintain the system at a constant temperature (25 ºC), and a digital laboratory stirrer (IKA Eurostar power control-visc) is used to control the agitation speed.

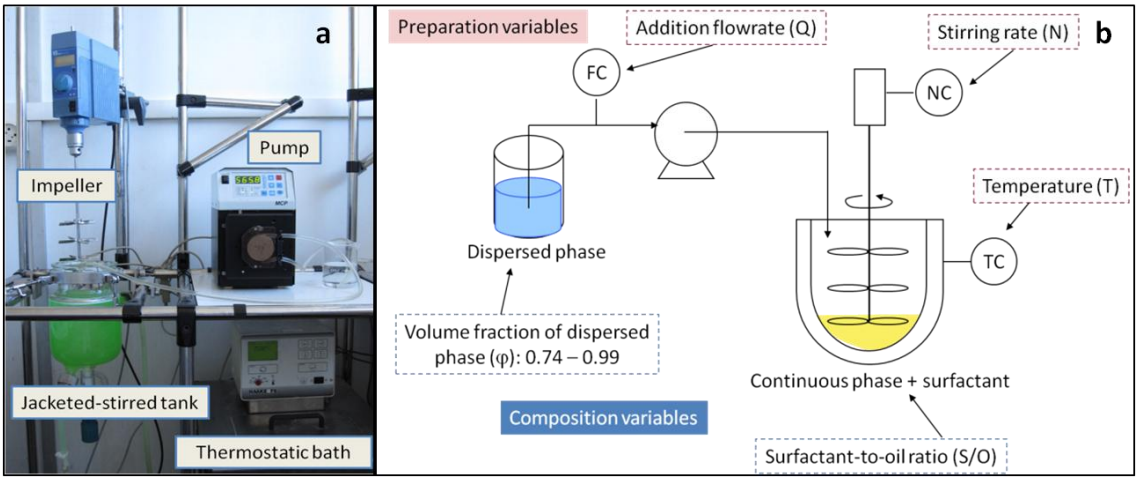

Figure 1. Installation to prepare the emulsions (a) photograph and (b) scheme.

During the first step, consisting of the dispersed phase incorporation, the continuous phase, formed by the surfactant and the oil, were weighed, mixed, and transferred into the reactor, which was already at the desired temperature. Values for the stirring rate (N, rpm) and for the addition flow rate (Q, mL/min) were chosen (according to the experiments planned) and at time $t = 0$, the agitation started and the dispersed phase (water) was added at the controlled and constant flow rate. The pump was calibrated before each experiment to ensure the precise value of the flow rate. The second step, corresponding to the homogenization of the emulsion, starts when the dispersed phase is

completely added. The emulsion is stirred then for 5 more minutes at the same stirring rate as in step 1 to ensure a good droplet breakup and incorporation of all the dispersed phase. With this method, reverse emulsions were formed easily and remained stable during a long period of time.

The torque (T) during emulsification was monitored with a IKA Eurostar power control-visc agitator. The parameters were set using the LabView software. From the torque and the stirring rate (N), the power (P) during emulsification was calculated and plotted as a function of time for each experiment. From these plots, different results could be obtained: the influence of the process variables on power consumption, and the energy consumption during emulsification (the area below the curves).

Two different scales with geometric similarity were used (1:2), in which the volume of the reactor is increased by 8 folds from small (70 mL) to medium scale (560 mL). This ratio was chosen since it is significant enough to detect the influence of the scale on the emulsion properties and, at the same time, to minimize the decrease of the surface area-to-volume ratio. A very large difference would involve a different predominant mechanism in the emulsification process: droplet breakup on the small scale and coalescence on the large scale (Tatterson, 1994). Each vessel has its own impeller, also fabricated following geometric similarity respect to the impeller diameter (D).

Table 2. Characteristic volume (V) and lengths of the system. V: emulsion volume, D: impeller diameter, B: vessel diameter, H: emulsion height.

Scale	V (mL)	D (cm)	B (cm)	H (cm)
Small	70	4.5	5	4
Medium	560	9	10	8

2.4 Experimental design

The experiments were designed according to a rotatable central composite design: 2^3 + star design. This methodology applied in this field allows a reduction of the number of experiments as well as the detection of possible interaction between factors. Moreover, the design chosen gives access to both the model curvature and to the representation of the results in response surfaces. Additionally, as a result of the data analysis, the main factors that have an influence on the desired property are detected and an empirical model is obtained. This model enables the prediction, through interpolation, of the system behavior and hence, of further experiments. The model can be validated by comparing the predicted values with the experimental ones. The statistical analysis of the data is performed with Statgraphics ® Plus (v. 4.1). The preparation and composition variables studied, which are the experimental factors, are three: the addition flow rate (*Q*) or total addition time (*t*), the stirring rate (*N*) and the surfactant concentration in terms of the ratio between surfactant and oil in the continuous phase (*S/O*). Figure 2 shows the scheme of the process, with the factors and response variables.

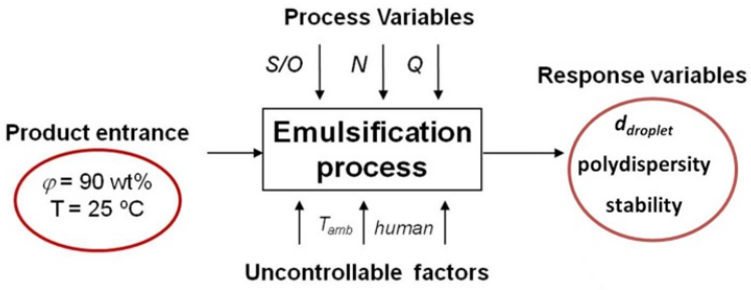

Figure 2. Diagram indicating the process, factors and response variables.

A total of 16 runs are needed in each scale, apart from the replicates: 8 (2^3) experiments correspond to the factorial design, at the high and low levels, 6 (2·3) experiments

correspond to the star points (at two extreme levels) and 2 experiments are the center points. The low and high levels, which are the same at both scales, and the center points, are shown in Table 3. The addition flow rate is related to the addition time by $t = V/Q$. As this emulsification time is constant in both scales, Q will differ, since the volume in both scales is different.

Table 3. Factors and levels studied.

Factors	Low	High	Center
S/O (wt/wt)	0.177	0.357	0.267
N (rpm)	700	1400	1050
t (min)	8.75	3.5	5
Q_1 (mL/min)	8	20	14
Q_2 (mL/min)	64	160	112

Although droplet size measurements were performed just after the emulsion was prepared, the emulsion stability was also checked in order to ensure that when the droplet size was determined, the emulsion had the same properties. Moreover, the stability is also an indication of the quality of the emulsification process and conditions chosen.

2.5 Determination of droplet size and polydispersity

Droplet size is determined from microphotographs taken with an optical microscope (Optika) equipped with a camera. Droplet size is calculated from more than 1000 diameter drops, which are measured on different microphotographs of the same emulsion. The measure of the diameter is performed with the Motic Images software, previously calibrated with standard images. All the microphotographs used to measure

372 the droplet size are made at 400x, in order to facilitate the measure of the drop diameter,
373 which is in the order of 1-10 μm. Droplet size is expressed as the Sauter mean diameter,
374 also known as the surface-weighted mean diameter ($d_{32} = \Sigma n_i \cdot d_i^3 / \Sigma n_i \cdot d_i^2$), since the
375 parameters describing the surface area are important in order to know the amount of
376 surfactant on the interface, for example. The number mean diameter (d_{10}) is also
377 evaluated. Polydispersity of an emulsion can be quantified using several parameters,
378 such as the standard deviation (s), used in this study, or the coefficient of variation (cv),
379 defined as the ratio of the standard deviation of the sample and the number mean
380 diameter ($cv = s/d_{10}$). When cv < 0.1, emulsions are considered to be monodisperse.
381
382 **3. Results and discussion**
383
384 **3.1 Characterization of the system used**
385 The analysis of the phase diagram showed that the system used does not present liquid
386 crystal regions in the emulsion formation path. The emulsions prepared had a micellar
387 continuous phase, which enabled their formation at room temperature (25 ºC). As the
388 volume fraction of dispersed phase (0.90) is higher than the packing of monodisperse
389 spheres (0.74), the emulsion droplets were in contact and presented polyhedral shapes.
390
391 **3.2 Influence of the process variables in droplet size**
392 The experimental runs, along with the droplet size and polydispersity, are found in the
393 Supporting Information (SI). The influence of the process variables was studied at both
394 scales. The Pareto charts shown in Figure 3 (small scale) and in Figure 4 (medium
395 scale) depict which factors and interactions have a significant effect on the response

variables. In the figure, the acronyms for the factors are the following: A for *S/O* (surfactant-to-oil ratio), B for *Q* (addition flow rate) and C for *N* (stirring rate). The two order factors are symbolized by AA, BB and CC (implying A^2, B^2 and C^2), and the interactions between the factors are symbolized as AB, AC and BC, for the interaction between *S/O* and *Q*, *S/O* and *N*, and *Q* and *N*, respectively. The significant effects, which are the ones with a p-value < significance level (0.05), are those who overcome the vertical line. The analysis of the results show that the stirring rate (C:*N*) is the factor that most influences the droplet size, in the range studied, followed by the surfactant concentration (A:*SO*). The interaction between both factors (AC), surfactant-to-oil ratio with stirring rate, appears to be significant at the small scale and not that much at the medium scale; and the stirring rate has a second-order effect, which is more relevant at the medium scale, as we will discuss later.

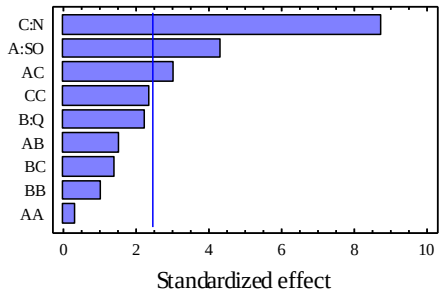

Figure 3. Standardized Pareto Chart for d_{32} (small scale).

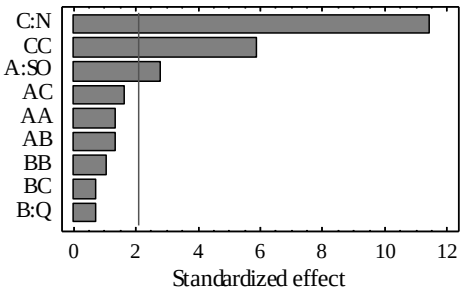

Figure 4. Standardized Pareto Chart for d_{32} (medium scale).

Quite similar patterns are obtained in both scales: droplet size decreases with increasing *N* and *S/O*, which is in agreement with other authors (Capdevila et al., 2010; Galindo-Rodríguez et al., 2005; Solè et al., 2010). As the higher values of *N* and *S/O* involve smaller droplet size, we can say that both factors have a negative effect on this property. When *N* increases, there is more energy to break up the dispersed phase into smaller droplets, and, as discussed in previous sections, *N* is related to the shear stress,

414 which is the force responsible for droplet breakup. On the other hand, when the
415 surfactant concentration increases, the interfacial area can increase, as there is more
416 surfactant to stabilize it, so droplets can be smaller.
417 From the analysis of the results, an empirical model that describes the behavior of the
418 system and expressed as $y = \beta_0 + \beta_1 \cdot x_1 + \beta_2 \cdot x_2 + \beta_{11} \cdot x_1^2 + \beta_{22} \cdot x_2^2 + \beta_{12} \cdot x_1 \cdot x_2 + \varepsilon$ is
419 determined (y is the response variable, x_i the factors, and β_i the model parameters). The
420 parameters of the equations and the regression coefficients are found in SI for both
421 scales and taking into account all the factors studied or just the ones that have a
422 significant effect (N, S/O, N^2 and $N \cdot S/O$ in the case of small scale, and N, S/O and N^2 in
423 the case of medium scale). The equations with the significant factors are shown below:
424 (1) for small scale and (2) for medium scale.
425
426 $$d_{32} = 33.48 - 52.57 \cdot S/O - 2.89 \cdot 10^{-2} N + 5.67 \cdot 10^{-6} \cdot N^2 + 3.67 \cdot 10^{-2} \cdot S/O \cdot N \quad (1)$$
427 $$d_{32} = 17.52 - 4.23 \cdot S/O - 1.92 \cdot 10^{-2} \cdot N + 7.00 \cdot 10^{-6} \cdot N^2 \quad (2)$$
428
429 These equations are used to generate the response surfaces, which show how the system
430 behaves. The response surfaces corresponding to the small scale experiments are shown
431 in Figs. 5-8 and the ones of the medium scale can be found in the SI. In order to see if
432 there is any difference with the models obtained taking into account all the factors (Fig.
433 5,7) and the ones obtained with only the significant factors (Fig. 6,8), both response
434 surfaces are generated. Moreover, as there are three factors, but we can only represent
435 two variables in each figure, in one figure, the Q is held constant at 14 mL/min
436 (although Figure 6, as Q appears not to be significant, would be the same for other

values of *Q*) to see the influence of *N* and *S/O* (Fig. 5,6) and in the other, to see the effect of *Q* and *S/O*, the stirring rate *N* is constant at 1050 rpm (Fig. 7,8).

As the model predicts, the influence of *S/O* to droplet size seems to be linear, whereas the effect of *N* is quadratic (Fig. 5,6). Moreover, at small scale the interaction between *S/O* and *N* has a significant effect: the influence of *N* is higher when the surfactant concentration is lower. There seems to be no difference between Figures 5 and 6 because, in this case, the variables observed and their interactions have a significant effect, which is far more important than the other interactions and second-order effects.

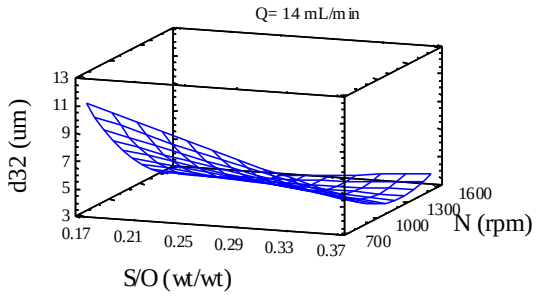

Figure 5. Estimated response surface for d_{32} (using the model with all factors) at small scale. Q constant at 14 mL/min.

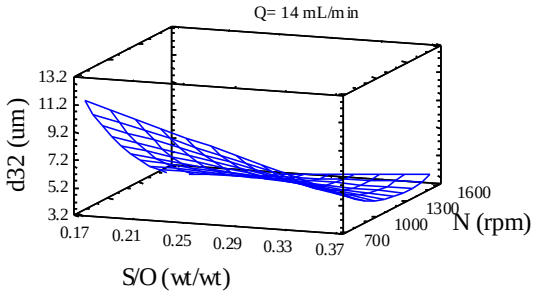

Figure 6. Estimated response surface for d_{32} (using the model with the significant factors: *N*, *S/O*, N^2, *S/O*·*N*) at small scale. Q constant at 14 mL/min.

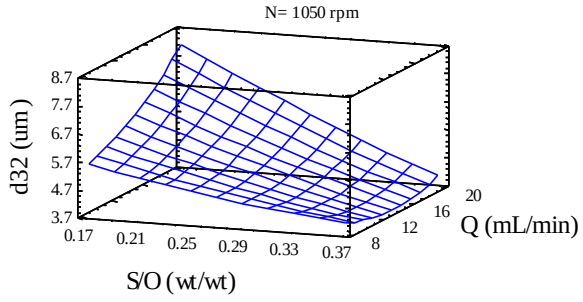

Figure 7. Estimated response surface for d_{32} (using the model with all factors) at small scale. N constant at 1050 rpm.

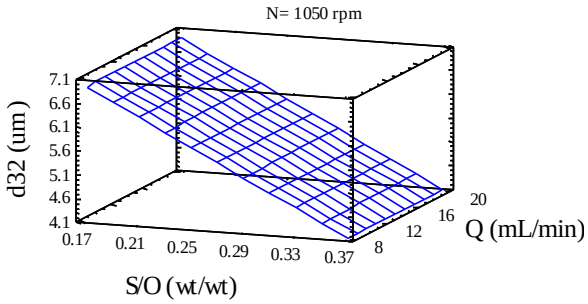

Figure 8. Estimated response surface for d_{32} (using the model with the significant factors: *N*, *S/O*, N^2, *S/O*·*N*) at small scale. N constant at 1050 rpm.

446 According to the analysis, and like in our previous study (Capdevila et al., 2010), the
447 addition flow rate (B:*Q*) appears to be not significant, as observed in the Pareto charts
448 (Figure 3,4) and in the normal probability plot (SI). However, by looking at Figure 7,
449 where the response surface is generated with the model obtained with all the possible
450 factors, and the effect of Q is depicted, we can observe that the influence of *Q* is quite
451 significant when the surfactant concentration is low: the higher the addition flow rate,
452 the bigger the droplet size. This is due to the fact that when the addition rate is high,
453 there is less time to break up the dispersed phase and bigger droplets are obtained,
454 which coalesce fast when there is not enough surfactant available. However, when
455 working at high surfactant concentration, this effect is balanced with the high amount
456 of amphiphile that can stabilize the system. If the response surface is represented with
457 only the significant factors (Figure 8), the effect of *Q* is not appreciated, since in this
458 case, the value of droplet size does not depend on *Q*, but only on *S/O* and *N* (since *Q*
459 does not appear in the model with only the significant factors). This happens both in
460 small and medium scale.
461
462 In this study, the validation of the model is performed by comparing the calculated
463 values obtained from the models with the experimental ones. Figure 9 shows the
464 validation of the models in both scales. The filled symbols are the points obtained
465 taking into account all the factors and interactions, and the open symbols are generated
466 taking into account only the significant ones. It can be observed that the points are near
467 the line $x = y$, which indicates that the model fits well to the experimental data.

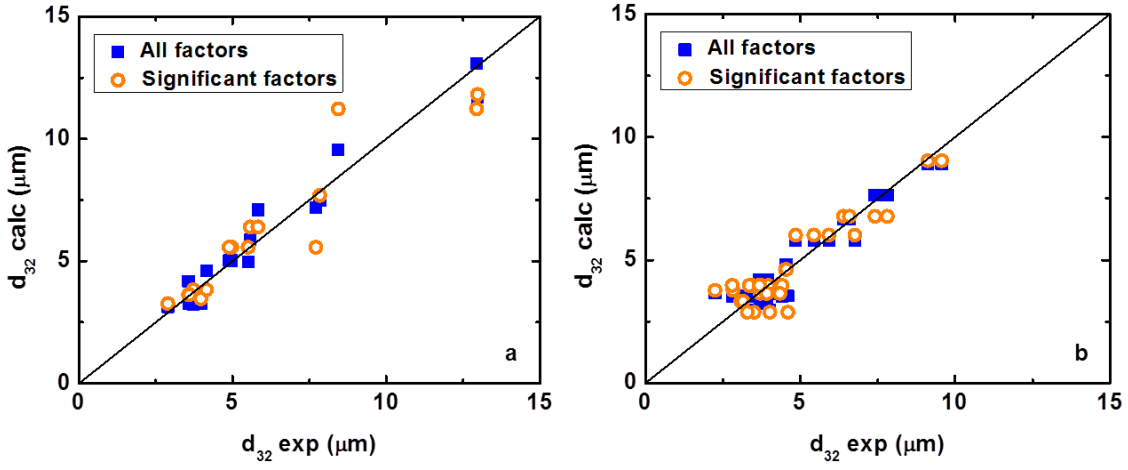

Figure 9. Plot of the calculated values versus the experimental results to validate the models: (**a**) small and (**b**) medium scales.

3.3 Scale-up following droplet size

The effect of the process variables in droplet size is similar on both scales. However, droplet size is found to be smaller at the medium scale, for the same values of the process variables, especially when *S/O* is low, *Q* high (*t* low) and *N* low. This indicates that at the medium scale, for the same values of *N*, there is more energy for droplet breakup. When the conditions are the opposite (*S/O* high and *Q* low, along all the range of *N*), the droplet sizes in both scales are quite similar, indicating that N could be a good scale invariant when these conditions are met.With the empirical models, the power law exponents of the scale invariants are found for each experimental condition, by minimizing the mean absolute error (MAE) (3) between the droplet size calculated with the medium scale model, and the one calculated for the small scale model, using a theoretical calculated stirring rate N_1 (4), which depends on the power law exponent. In equation (3), *n* is the number of points used; in this case $n = 26$, since values from $N = 350$ rpm to 1600 rpm are taken, in intervals of 50 rpm.

$$MAE = \frac{1}{n}\sum_{i=1}^{n} |d_{32}(calc, medium\ scale) - d_{32}(calc, small\ scale)| \quad (3)$$

$$N_1 = N_2 \cdot (D_2/D_1)^{\alpha} \quad (4)$$

The representations of the droplet size obtained with both empirical models and with the equation obtained by minimizing the MAE are shown in Figure 10, as a function of *N*, at different experimental conditions (varying *S/O* and *Q* (or *t*)).

When the values of the process variables involve that the droplet sizes in both scales are similar, the power law exponent obtained in the scale invariant analysis is close or equal to 0, indicating that *N* is the proper scale invariant in those conditions, as our previous study indicated (Capdevila et al., 2010) and confirming the experimental results. However, as *S/O* decreases and *Q* increases, the difference between both scales increases and the power law exponent reaches values of 0.5, indicating that in these conditions *N* is not the proper scale invariant.

Apart from the empirical models, the experimental results for both scales are also depicted in Figure 10. It can be observed that at the small scale, the droplet diameter is bigger, especially when the surfactant concentration and the addition time are low (Figure 10,d,f). When the surfactant concentration and the addition time are high, and when $N > 1500$ rpm, there is no difference in droplet size, so $\alpha \rightarrow 0$ (Figure 10,c,g).

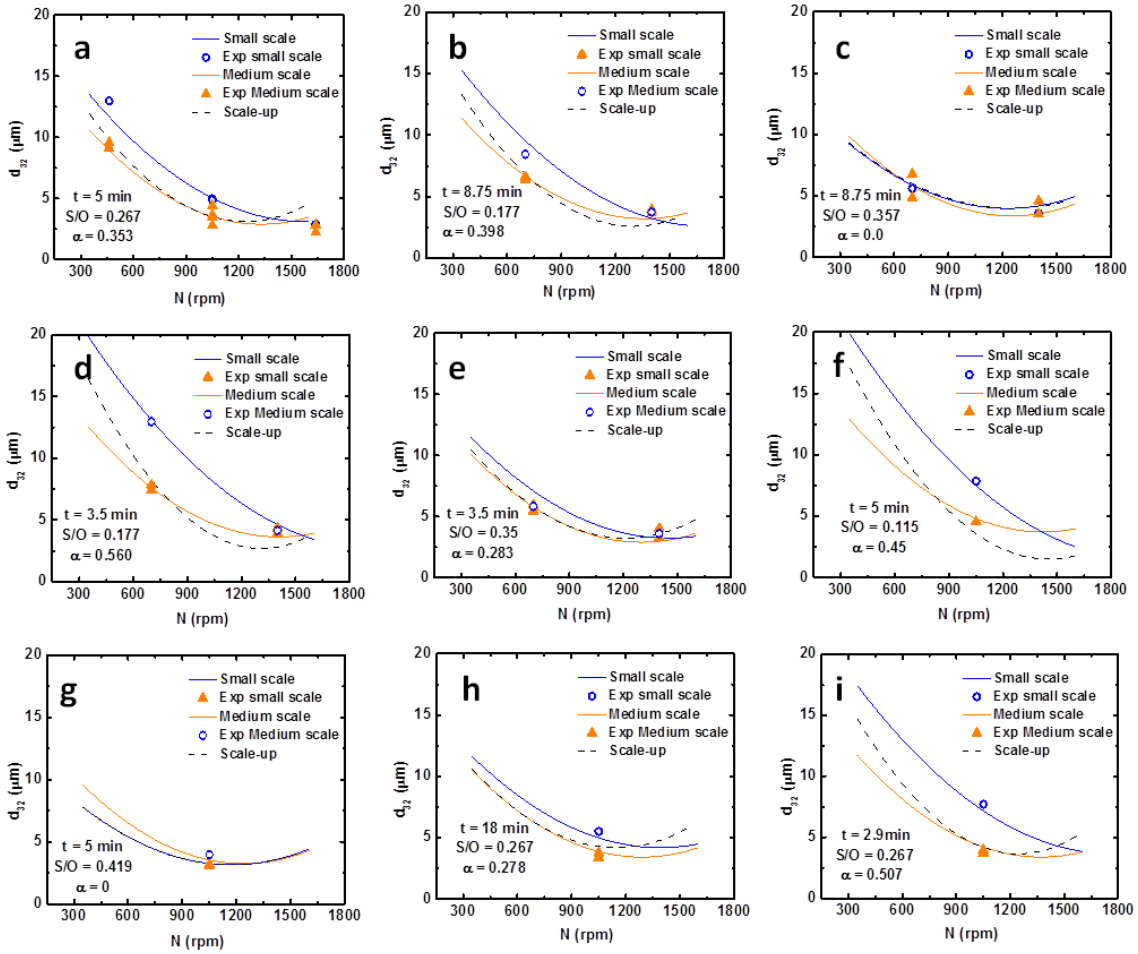

Figure 10. Droplet size as a function of *N*, for different values of *S/O* and *t*. The continuous lines represent the empirical model found (including all factors) at both scales, and the dashed line, the small scale droplet size calculated at a stirring rate using the optimum power law exponent ($N_1 = N_2 \cdot (D_2/D_1)^{\alpha}$).

Figure 11 shows the change in the power law exponent with *S/O* and addition time. Each value is valid for the whole range of *N* (from 350 to 1600 rpm).

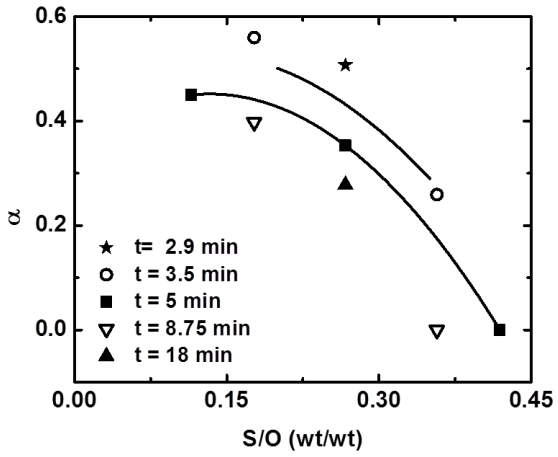

Figure 11. Evolution of the power law exponent with *S/O* at different total addition times of emulsification. The five addition-time levels correspond to the factorial, center and star points.

We can see that when the surfactant concentration is low, the power law exponent is around 0.5, whereas the higher the surfactant concentration, the lower the power law exponent, which approaches 0, especially when the addition time increases. This indicates that at a high surfactant concentration and when the dispersed phase has more time to breakup in smaller droplets, the stirring rate seems to be a proper scale invariant. In fact, the emulsions obtained at these conditions are the most stable ones, and their droplet size is smaller. The threshold values for N as a scale invariant would be $S/O > 0.5$ and $t > 5$ min. On the other hand, when the surfactant concentration is lower, the emulsions obtained have bigger droplet sizes and are less stable. In this case, the scale invariant approaches $N \cdot D^{0.5}$, which, according to Table 1, indicates that what is relevant is a constant surface motion. To be sure of performing a proper scale-up, we propose to determine in which conditions the power law exponent approximates 0, and to establish these conditions along with addition time and stirring rate as invariants in the scaling-up process. As it has been said, the power law exponent, 0 in this case, would be valid for a wide range of N, from 350 up to1600 rpm.

3.4 Influence of the process variables and scale-up following polydispersity

The polydispersity of the emulsion, calculated as the standard deviation of droplet size, followed the same behavior as droplet size (Figures in SI). At both scales, the factors that most influenced polydispersity are the stirring rate, in quadratic form, and the *S/O*. There is also an interaction between both factors. The addition flow rate, as in droplet size, is not a significant factor, although its influence is important when the surfactant concentration is low, increasing the polydispersity when *Q* is high.

3.5 Influence of the process variables on power consumption

The influence of the process variables is reflected in the power consumption at both scales. At small scale, the power appears to be independent of the water flow rate (*Q*) at a given *N* and *S/O* (Figure 12-a); it increases with agitation speed at a given *Q* and *S/O* (Figure 12-b), and *S/O* has a minor influence, at a given *N* and *Q* (Figure 12-c). Hence, the stirring rate is the parameter that most increments the energy consumption, as it can be expected. Another observation in the small scale is that the power consumption is constant or nearly constant from the beginning to the end of the test, and there is no big difference between the two emulsification steps (addition and homogenization).

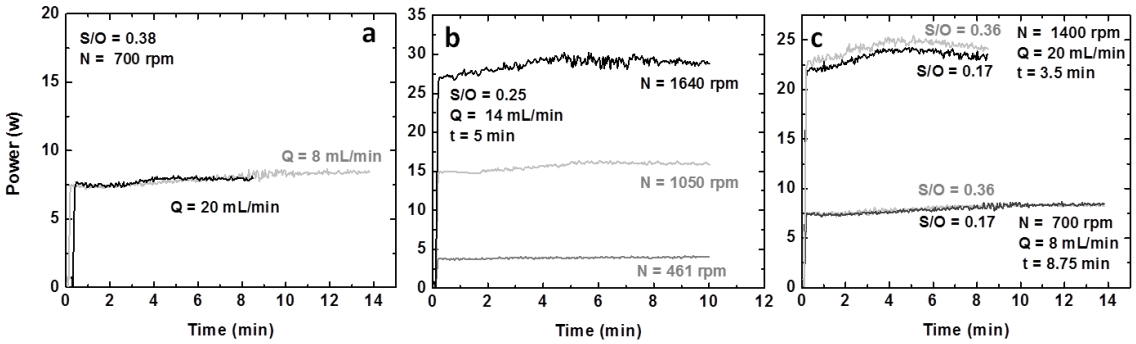

Figure 12. Power evolution with time at (a) different *Q*, (b) different *N* and (c) different *S/O* (small scale).

In the medium scale, we can observe that, unlike in the small scale, the power consumption is divided in two different areas: in step 1, where the addition of dispersed phase takes place, the power increases with time, and in step 2, where the homogenization of the emulsion takes place, the power consumption remains constant (Figure 13). The fluctuations observed are possibly due to errors in the data acquisition or transmission. As happened in the small scale, the main parameter that has an influence in the power consumption is the stirring rate (Figure 13-b). However, the influence of Q is also significant: when working at 193 mL/min, the power consumption increases significantly in step 1, and then remains constant at 30 w, whereas when working at 31 mL/min, the power consumption increases at a lower rate and then remains constant at around 25 w (Figure 14-a). In the case of *N*, the difference is bigger: when working at 461 rpm, the power consumption is constant at 5 w, whereas at 1050 rpm, the power increases up to 25 w, and at 1639 rpm, the power reaches 45 w. The *S/O*, in the range studied, does not have a significant influence (Figure 13-c).

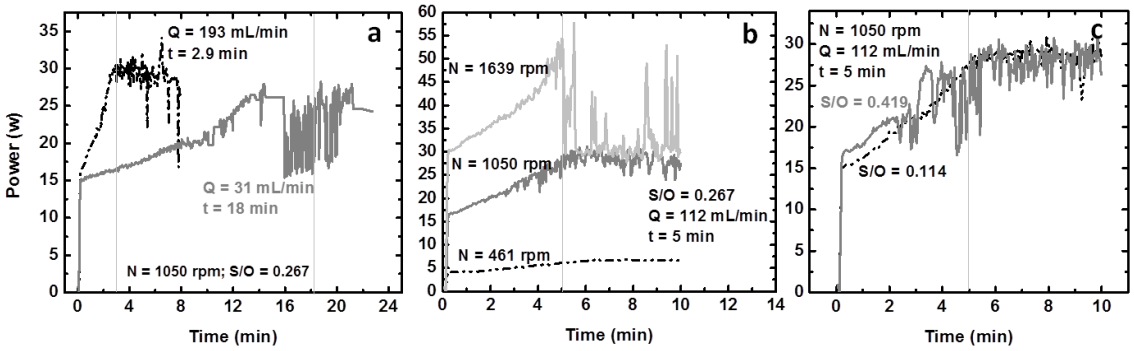

Figure 13. Power evolution with time at (a) different *Q*, (b) different *N* and (c) different *S/O* (medium scale).

Figure 14 exemplifies the difference in power consumption in the formation of emulsions at both scales. We can see that at small scale, from the first moment to the end, the power remains constant, whereas in the medium scale, the power consumption increases during step 1, corresponding to the addition time of dispersed phase, and then remains constant during the homogenization step (step 2).

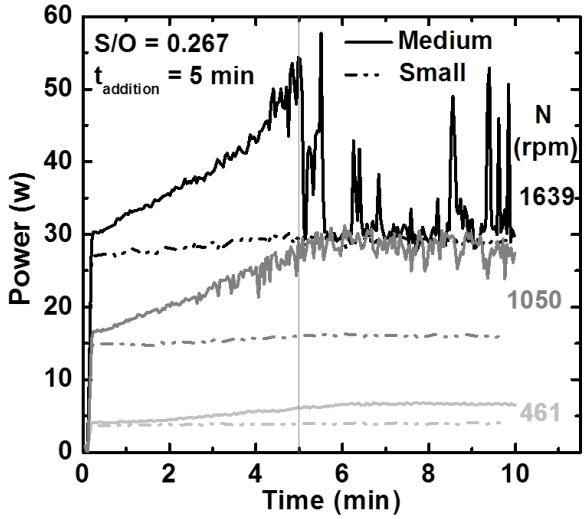

Figure 14. Power consumption along the emulsification time in emulsions formed with S/O = 0.267, t_{add} = 5 min, at three different N (461, 1050, 1639 rpm) for small scale (dashed line) and medium scale (continuous line).

4. Conclusions

In the range studied, the surfactant concentration (*S/O*) and the stirring rate (*N*) were found to be the main factors that influenced droplet size, polydispersity and power consumption. In general, at higher *N* and *S/O*, emulsions have a smaller droplet size with less polydispersity. The power consumption is higher at the medium scale. Moreover, in this scale, it increases in step 1 and remains constant in step 2, whereas in the small scale, there is no difference between the two steps.

The empirical models relating the process variables with the emulsion properties were obtained and used in the scale-up analysis. The scale-up is performed by keeping the stirring rate and the total addition time of dispersed phase as invariant in both scales experiments. A higher value of the droplet size is obtained at a smaller scale for nearly all the experimental conditions tested, showing that stirring rate is not the adequate invariant in scaling-up. Other scale-up invariants were required, which presented the form $N_i \cdot D_i^{\alpha}$. A different power law exponent (α) could be determined when changing the experimental conditions, as an approximation to the scale-up invariants for this system. Although there is no scale invariant valid for all the range of the process variables studied, a correlation between this exponent and the process variables is found. According to the results obtained, when the stirring rate is high enough, or when *S/O* and t are high, $\alpha \rightarrow 0$; otherwise, the power law exponent increases.

These results justify that different authors propose different scale-up criteria as can be seen in Table 1: the power law exponent changes depending on the system and on the conditions. Studies for scaling-up specific systems should include the determination of the power law exponent applicable to this system and, if it is considered convenient for a safer scale-up, the determination of conditions where the exponent is approximately constant when the other variables are changing.

5. Acknowledgements

This research was supported by the Ministry of Economy and Competitiveness (MINECO) of the Spanish Government (project CTQ2011-29336-C03-02).

6. Appendix A. Supporting information

Supplementary data associated with this article can be found in the online version at http://dx.doi.org/10.1016/j.ces.2013.07.033.

7. References

Alvarez, O.A., 2006. Emulsions inverses très concentrées. Influence du procedé et de la formulation sur leurs proprietes rhéologiques. École Nationale Supérieure des Industries Chimiques.

Alvarez, O.A., Choplin, L., Sadtler, V., Marchal, P., Stébé, M.-J., Mougel, J., Baravian, C., 2010. Influence of semibatch emulsification process conditions on the physical characteristics of highly concentrated water-in-oil emulsions. Industrial & Engineering Chemistry Research 49, 6042–6046.

Angst, R., Kraume, M., 2006. Experimental investigations of stirred solid/liquid systems in three different scales: Particle distribution and power consumption. Chemical Engineering Science 61, 2864–2870.

Anne-Archard, D., Marouche, M., Boisson, H.C., 2006. Hydrodynamics and Metzner–Otto correlation in stirred vessels for yield stress fluids. Chemical Engineering Journal 125, 15–24.

Baby, A.R., Santoro, D.M., Velasco, M.V.R., Dos Reis Serra, C.H., 2008. Emulsified systems based on glyceryl monostearate and potassium cetyl phosphate: scale-up and characterization of physical properties. International Journal of Pharmaceutics 361, 99–103.

Bakker, A., Gates, L.E., 1995. Properly choose mechanical agitators for viscous liquids. Chemical Engineering Progress 91, 25–34.

Baldyga, J., Bourne, J.R., Pacek, A.W., Amanullah, A., Nienow, A.W., 2001. Effects of agitation and scale-up on drop size in turbulent dispersions: allowance for intermittency. Chemical Engineering Science 56, 3377–3385.

Bird, B., Stewart, W.E., Lightfoot, E.N., 1964. Transport Phenomena. John Wiley and Sons, New York.

Bourne, J.R., Yu, S., 1994. Investigation of micromixing in stirred tank reactors using parallel reactions. Industrial & Engineering Chemistry Research 33, 41–55.

Briceño, M.I., Salager, J.-L., Bertrand, J., 2001. Influence of dispersed phase content and viscosity on the mixing of concentrated oil-in-water emulsion in the transition flow regime. Trans IChemE 79.

649 Capdevila, M., Maestro, A., Porras, M., Gutiérrez, J.M., 2010. Preparation of Span
650 80/oil/water highly concentrated emulsions: influence of composition and
651 formation variables and scale-up. Journal of Colloid and Interface Science 345,
652 27–33.

653 Dickey, D.S., 2005. Don't get mixed up by scale-up [WWW Document]. Chemical
654 Processing. URL http://www.chemicalprocessing.com/articles/2005/519/ (accessed
655 2.19.13).

656 Galindo-Rodríguez, S.A., Puel, F., Briançon, S., Allémann, E., Doelker, E., Fessi, H.,
657 2005. Comparative scale-up of three methods for producing ibuprofen-loaded
658 nanoparticles. European Journal of Pharmaceutical Sciences 25, 357–67.

659 Gorsky, I., 2006. Parenteral drug scale-up, in: Dekker, M.I. (Ed.), Pharmaceutical
660 Process Scale-up. Taylor & Francis, New York, pp. 43–56.

661 Gutiérrez, J.M., González, C., Maestro, A., Solè, I., Pey, C.M., Nolla, J., 2008. Nano-
662 emulsions: New applications and optimization of their preparation. Current
663 Opinion in Colloid & Interface Science 13, 245–251.

664 Houcine, I., Plasari, E., David, R., 2000. Effects of the stirred tank's design on power
665 consumption and mixing time in liquid phase. Chemical Engineering &
666 Technology 23, 605–613.

667 Johnson, R.T., 1967. Batch mixing of viscous liquids. Industrial & Engineering
668 Chemistry Process Design and Development 6, 340–345.

669 Landin, M., York, P., Cliff, M.J., Rowe, R.C., Wigmore, A.J., 1996. Scale-up of a
670 pharmaceutical granulation in fixed bowl mixer-granulators. International Journal
671 of Pharmaceutics 133, 127–131.

672 Levin, M., 2006. Pharmaceutical process scale-up, Second Edi. ed. Taylor & Francis,
673 New York.

674 Metzner, A.B., Otto, R.E., 1957. Agitation of non-Newtonian fluids. AIChE Journal 3,
675 3–10.

676 Mitri, K., Vauthier, C., Huang, N., Menas, A., Ringard-Lefebvre, C., Anselmi, C.,
677 Stambouli, M., Rosilio, V., Vachon, J.-J., Bouchemal, K., 2012. Scale-up of
678 nanoemulsion produced by emulsification and solvent diffusion. Journal of
679 Pharmaceutical Sciences 101, 4240–4247.

680 Okufi, S., Ortiz, D., Perez, E.S., Sawistowski, H., 1990. Scale-up of liquid-liquid
681 dispersions in stirred tanks. The Canadian Journal of Chemical Engineering 68,
682 400–406.

683 Podgórska, W., Baldyga, J., 2001. Scale-up effects on the drop size distribution of
684 liquid-liquid dispersions in agitated vessels. Chemical Engineering Science 56,
685 741–746.

686 Rewatkar, V.B., Joshi, J.B., 1991. Effect of impeller design on liquid phase mixing in
687 mechanically agitated reactors. Chemical Engineering Communications 102, 1–33.

688 Solè, I., Pey, C.M., Maestro, A., González, C., Porras, M., Solans, C., Gutiérrez, J.M.,
689 2010. Nano-emulsions prepared by the phase inversion composition method:
690 preparation variables and scale up. Journal of Colloid and Interface Science 344,
691 417–23.

692 Tatterson, G.B., 1994. Scaleup and Design of Industrial Mixing Processes, Mc-Graw
693 Hi. ed. New York.

694 Taylor, R.A. (Tony), Penney, W.R., Vo, H.X., 2005. Scale-up methods for fast
695 competitive chemical reactions in pipeline mixers. Industrial & Engineering
696 Chemistry Research 44, 6095–6102.

697 Thakur, R.K., Vial, C., Djelveh, G., Labbafi, M., 2004. Mixing of complex fluids with
698 flat-bladed impellers: effect of impeller geometry and highly shear-thinning
699 behavior. Chemical Engineering and Processing: Process Intensification 43, 1211–
700 1222.

701 Wilkens, R.J., Henry, C., Gates, L.E., 2003. How to scale-up mixing processes in non-
702 Newtonian fluids. Chemical Engineering Progress 99, 44–52.

703 Wilkens, R.J., Miller, J.D., Plummer, J.R., Dietz, D.C., Myers, K.J., 2005. New
704 techniques for measuring and modeling cavern dimensions in a Bingham plastic
705 fluid. Chemical Engineering Science 60, 5269–5275.

706 Zlokarnik, M., 1998. Problems in the application of dimensional analysis and scale-up
707 of mixing operations. Chemical Engineering Science 53, 3023–3030.

708
709
710 **Published in**: Chemical Engineering Science, Volume 101, 20 September 2013, Pages 721–730

711